

## Research Article

# Identification of Immune-Related lncRNAs for Predicting Prognosis and Immune Landscape Characteristics of Uveal Melanoma

Wei Chen, Liying Yan, Bo Long, and Li Lin 

Department of Ophthalmology, Suining Central Hospital, No. 127, West Desheng Road, Chuanshan District, Suining 629000, Sichuan Province, China

Correspondence should be addressed to Li Lin; [vivalinli@hotmail.com](mailto:vivalinli@hotmail.com)

Received 1 July 2022; Revised 18 July 2022; Accepted 2 August 2022; Published 29 August 2022

Academic Editor: Jinghua Pan

Copyright © 2022 Wei Chen et al. This is an open access article distributed under the Creative Commons Attribution License, which permits unrestricted use, distribution, and reproduction in any medium, provided the original work is properly cited.

Immune-related genes and long noncoding RNAs (lncRNAs) have a significant impact on the prognostic value and immunotherapeutic response of uveal melanoma (UM). Therefore, we tried to develop a prognostic model on the basis of irlncRNAs for predicting prognosis and response on immunotherapy of UM patients. We identified 1,664 immune-related genes and 2,216 immune-related lncRNAs (irlncRNAs) and structured a prognostic model with 3 prognostic irlncRNAs by co-expression analysis, univariable Cox, LASSO, and multivariate Cox regression analyses. The Kaplan–Meier analysis indicated that patients in the high-risk group had a shorter survival time than patients in the low-risk group. The ROC curves demonstrated the high sensitivity and specificity of the signature for survival prediction, and the one-, three-, and five-year AUC values, respectively, were 0.974, 0.929, and 0.941 in the entire set. Cox regression analysis, C-index, DCA, PCA analysis, and nomogram were also applied to assess the validity and accuracy of the risk model. The GO and KEGG enrichment analyses indicated that this signature is significantly related to immune-related pathways and molecules. Finally, we investigated the immunological characteristics and immunotherapy of the model and identified various novel potential compounds in the model for UM. In summary, we constructed a new model on the basis of irlncRNAs that can accurately predict prognosis and response on immunotherapy of UM patients, which may provide valuable clinical applications in antitumor immunotherapy.

## 1. Introduction

Uveal melanoma (UM) is the commonest primary intraocular malignancy in adults, contributing up to 85% of ocular melanomas, and more than half of individuals with UM experience systemic metastatic disease [1, 2]. UM mainly originates from the choroid, iris, and ciliary body and has a prevalence of 5.1 per million in America [3, 4]. Over the past 30 years, although local treatments for UM have been developed, 5-year survival rates have not changed, and no effective complementary therapy is currently available to decrease the risk of metastasis from UM [5, 6]. In addition, because of the high heterogeneity of UM, patients with identical stages receive similar treatment but showed very diverse prognostic outcomes [7]. Hence, the identification of

dependable prognostic biomarkers is essential for personalized treatment.

Noticeably, immunotherapy remarkably improved the prognosis of patients with cutaneous melanoma, yet poorly improved UM [4]. Previous retrospective studies have shown a low immune response rate to immunotherapy in UM patients, such as 10–21% for the combination of ibrutinomab and nilumab, 3.6% for anti-PD-1 antibodies, and 5% for ibrutinomab monotherapy [8–12]. Long noncoding RNAs (lncRNAs) are engaged in tumor cell proliferation, invasive metastasis, apoptosis, drug resistance, immune escape, and so on due to their influence on oncogenes and oncogenes of tumors [13, 14]. Therefore, lncRNAs are considered a highly promising candidate for personalized medicine for UM patients as a biomarker as well as a potential therapeutic target.

In this research, we identified the immune-related lncRNAs (irlncRNAs) and developed a risk assessment model by using univariable Cox, LASSO, and multivariate Cox regression analyses. Also, we evaluated the immunological atlas and found a variety of new potential therapeutic drugs in the model. In summary, we developed a risk assessment model for UM on the basis of irlncRNAs that can predict the prognosis and immunotherapy response in UM patients.

## 2. Methods and Materials

**2.1. Preparation of Data.** RNA-seq data and clinical information for UM were gathered using The Cancer Genome Atlas (TCGA, <https://tcga-data.nci.nih.gov/tcga>). Annotations based on the Ensembl database (<http://asia.ensembl.org>) were used to derive mRNA and lncRNA expression patterns. The ImmPort database (<http://www.immport.org>) was utilized to derive the expression patterns of immune-related genes. In order to identify irlncRNAs, the  $\text{cor} > 0.4$  and  $p < 0.001$  criteria were applied using the R package *limma*.

**2.2. Establishment of Risk Assessment Model.** A training subset and a test subset were created from the whole TCGA dataset. The whole set was utilized to identify prognosis of irlncRNAs, LASSO regression analysis was used to filter these prognosis of irlncRNAs, and multivariate Cox regression analysis was used to examine the remaining prognosis of irlncRNAs, resulting in a prognostic risk model. Each patient had a unique risk score, which was determined using the following formula:  $\sum_{i=1}^k \beta_i s_i$ . UM patients were assigned to high- and low-risk groups on the basis of their median risk score.

**2.3. Validation of Prognostic Model.** The Kaplan–Meier analysis was performed to compare the survival rates of the high-risk and low-risk groups. The area under the curve (AUC) and time-dependent receiver-operating characteristic (ROC) curves were applied to assess the model's ability to predict survival when compared to standard clinicopathological features. Cox analyses, both univariate and multivariate, were utilized to confirm that the model was an independent determinant of prognosis. To examine the model's accuracy in comparison to standard clinicopathological features, the concordance index (C-index) and decision curve analysis (DCA) were used. A nomogram integrating prognostic signatures was constructed to predict the one-, three-, and five-year survival rates of patients. The whole gene expression profiles, immune-genes, irlncRNAs, and the irlncRNAs in the model were subjected to a principal component analysis (PCA) study for exploratory display of high-dimensional data.

**2.4. Exploration of Immunological Atlas.** The Gene Ontology (GO)  $p < 0.05$  and Kyoto Encyclopedia of Genes and Genomes (KEGG)  $p < 0.05$  enrichment analyses for

differentially expressed genes were used to investigate possible causes of prognostic variations in various risk categories. In order to obtain a valid assessment of immune infiltration, we employed the current established methodologies, including xCELL, TIMER, quanTIseq, MCP-counter, EPIC, CIBERSORT-ABS, and CIBERSORT. In our study, Wilcoxon signed rank test was used to compare the expression levels of immune checkpoint inhibitors (ICIs)-related molecules between groups. Single-sample gene set enrichment analysis (ssGSEA) was used to determine whether immune function differed between groups. Using the tumor immune dysfunction and exclusion (TIDE) method, we were able to predict the variation in immunotherapeutic responses between groups.

**2.5. Identification of Potential Drugs.** Based on the Genomics of Drug Sensitivity in Cancer (GDSC, <https://www.cancerrxgene.org>), we calculated the half inhibitory concentration (IC50) of compounds. In addition, we used Wilcoxon signed rank testing to identify potential compounds for UM treatment in the clinic based on the difference in IC50 between different groups.

## 3. Results

**3.1. Identification of Immune-Related lncRNAs.** TCGA was employed to acquire RNA-seq data and clinical information for UM, which included 80 tumor samples. On the basis of the given data, we extracted expression profiles for 1,664 immune-related genes and 16,876 long noncoding RNAs. As a result of the co-expression analysis, 2,216 irlncRNAs were identified ( $\text{cor} > 0.4$  and  $p < 0.001$ ).

**3.2. Construction of Prognostic Risk Model.** Based on a ratio of 1:1, the entire TCGA set (80 samples) was randomly allocated to a training set (40 samples) and a testing set (40 samples), and a risk model was built by the entire set. We screened 409 prognostic irlncRNAs using univariate Cox regression analysis from a total of 2,216 irlncRNAs ( $p < 0.05$ ; Supplementary Table 1). The LASSO regression analysis was utilized to filter out 6 candidate irlncRNAs from a total of 409 prognostic irlncRNAs, as shown in Figures 1(a) and 1(b), with the associated LASSO coefficient profiles and a partial likelihood deviation plot. Finally, a risk assessment model on the basis of multivariate Cox regression analysis was developed, which incorporated 3 irlncRNAs (AP005121.1, AC104117.3, and SOX1-OT; Figure 1(c)). Supplementary Table 2 demonstrates the baseline features of these datasets, with no statistically significant variations in clinical features ( $p > 0.05$ ).

**3.3. Validation of Risk Assessment Model.** The survival analysis, irlncRNA expression profiles, pattern of survival status, and distribution of risk grades between different groups were described in the entire set (Figures 1(d) and 1(e)), the training set (Supplementary Figure 1(a)), and the testing set (Supplementary Figure 1(b)), indicating that

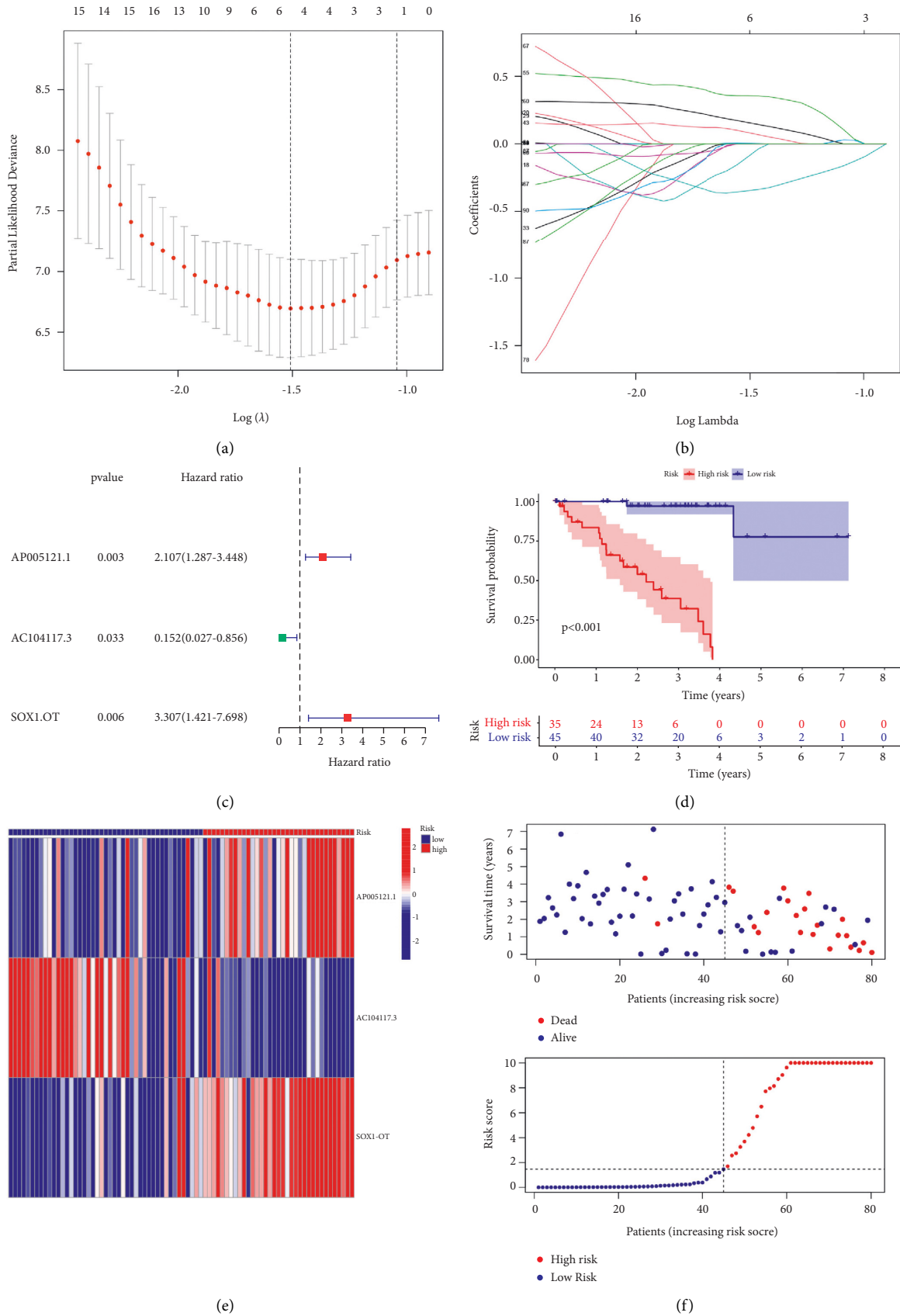


FIGURE 1: (a) LASSO coefficient profiles. (b) Coefficient profile plot generated against the log sequence. (c) 3 prognostic irlncRNAs identified by multivariate Cox regression analysis. (d) Kaplan-Meier survival curve of the model in the entire set. (e) The expression of the 3 prognostic irlncRNAs, patterns of survival outcome, and distribution of risk score for patients between different groups in the whole set.

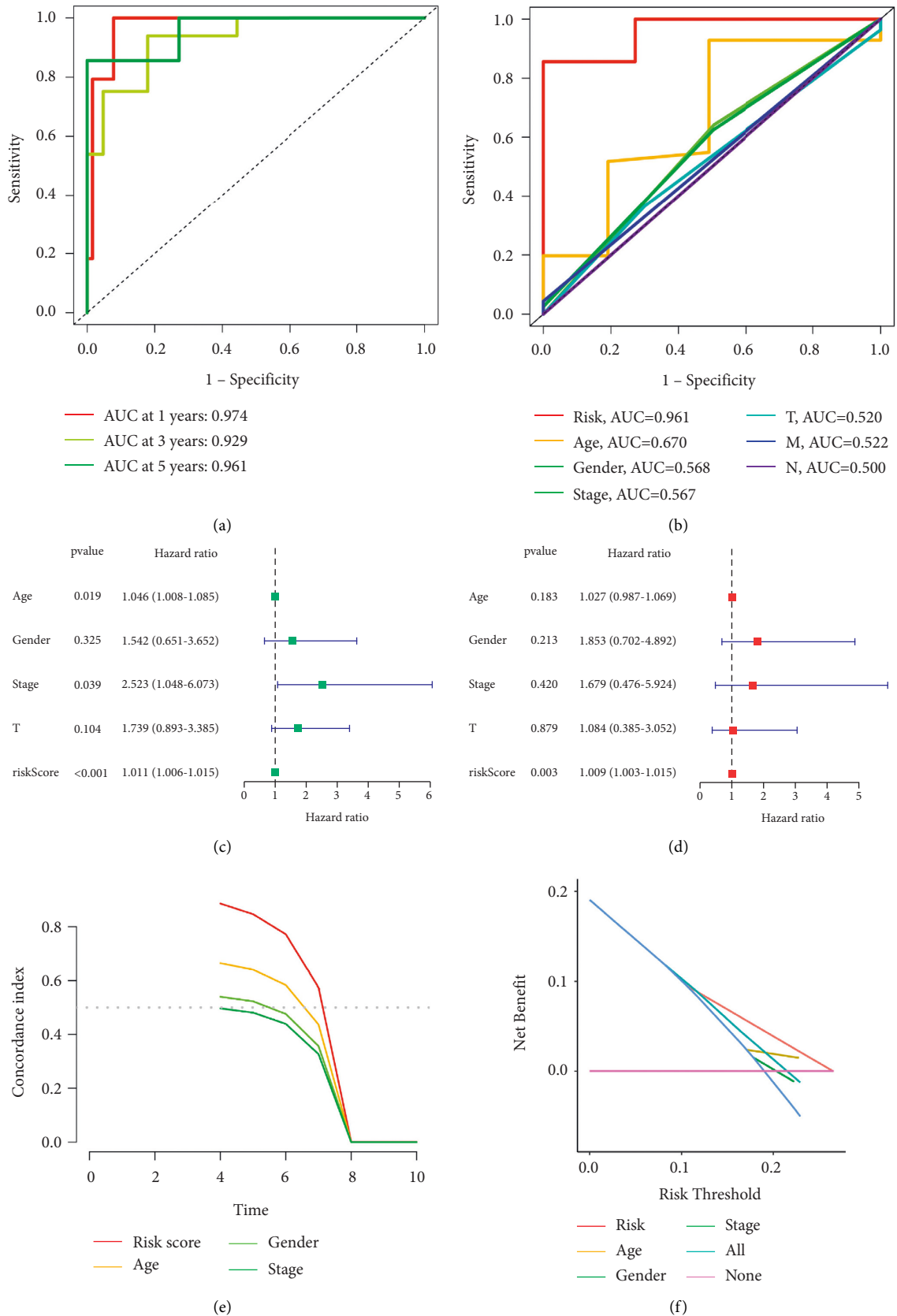


FIGURE 2: (a) One-, three-, and five-year AUC values, respectively, were 0.974, 0.929, and 0.941 in the entire set. (b) The five year AUC values of the model were higher than the traditional clinicopathological characteristics. (c) Univariate Cox regression analysis demonstrated that risk score was statistically associated with prognosis. (d) Multivariate Cox regression analysis showed that the risk score was an individual prognostic risk factor. (e, f) The C-index and DCA demonstrated that the signature better forecasted the prognosis of UM than other traditional clinicopathological characteristics.

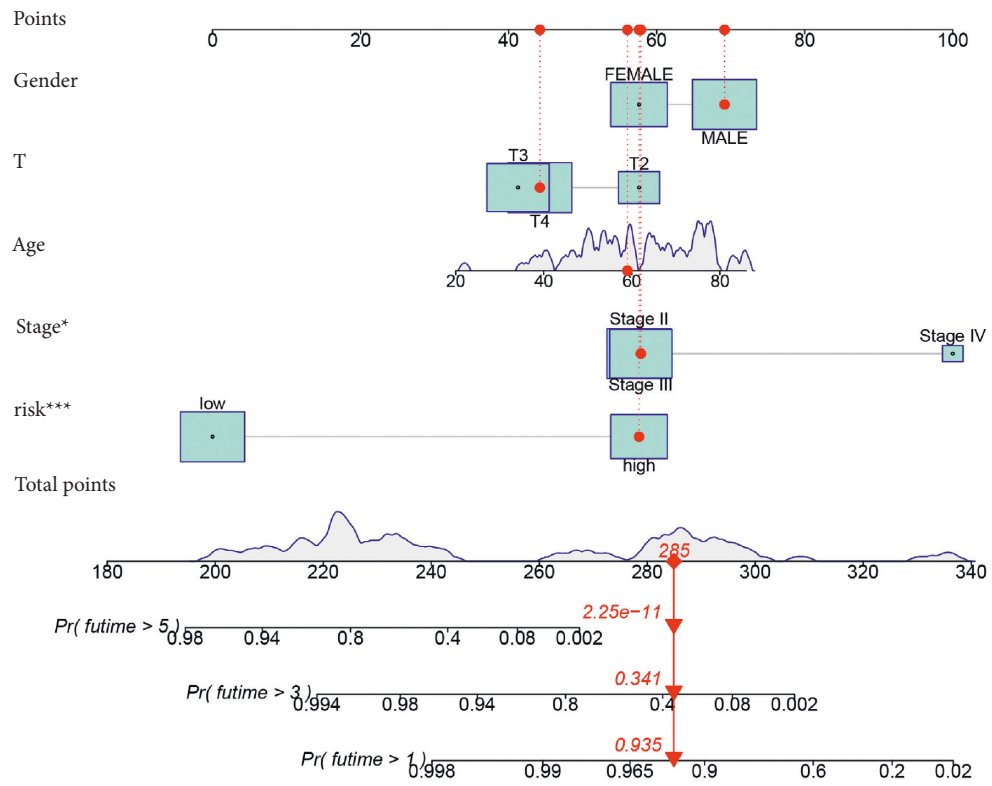


FIGURE 3: A nomogram including the model and clinicopathological characteristics was reliable and sensitive and can be applied to predict UM patient survival.

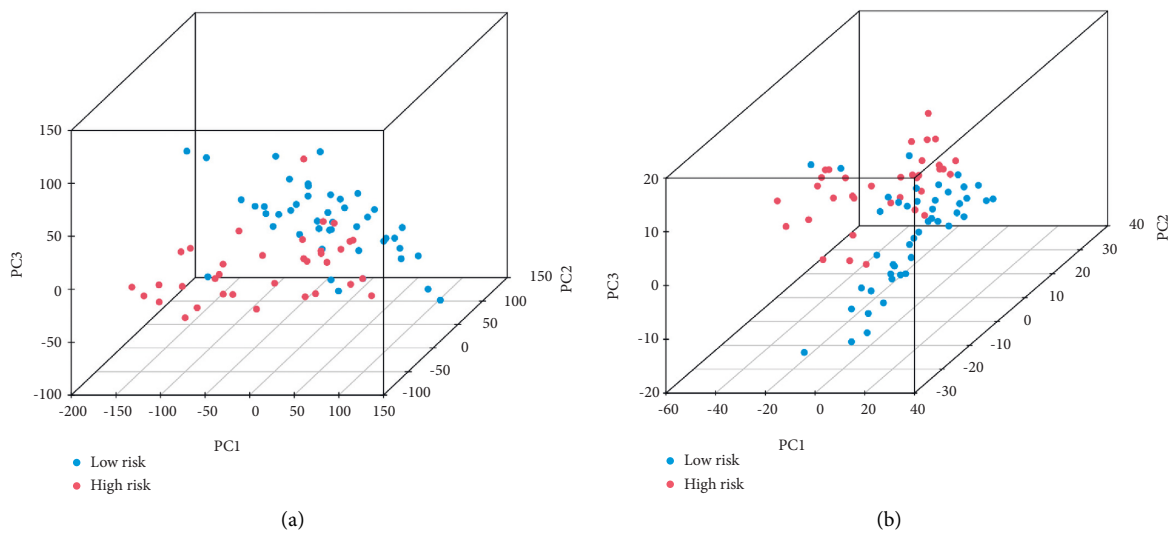


FIGURE 4: Continued.

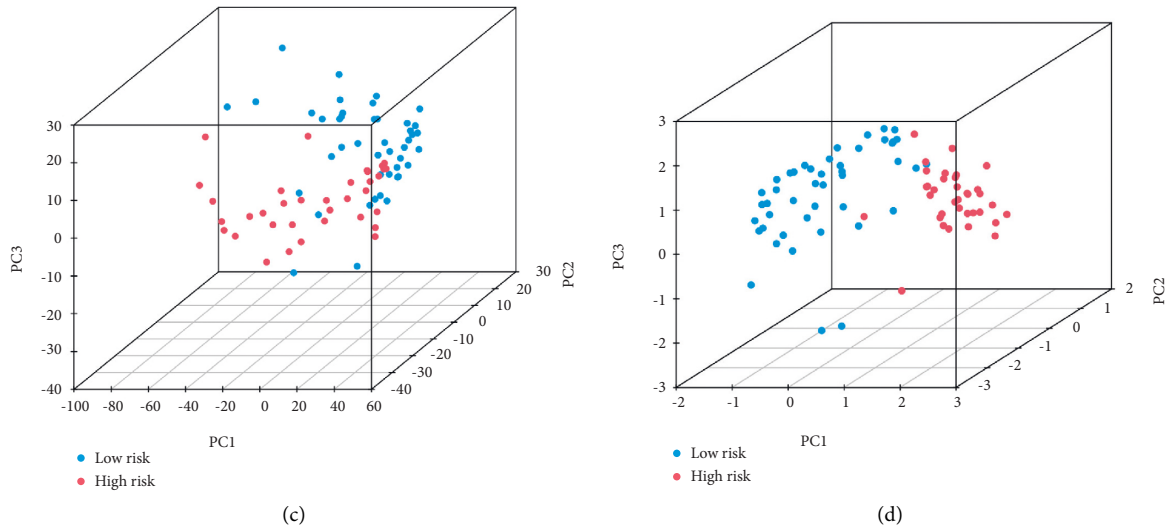


FIGURE 4: (a–d) PCA indicated that the distributions of entire gene expression profiles, immune-related genes, and irlncRNAs between different groups were relatively scattered, while the distributions of 3 irlncRNAs in the signature between different groups had different distributions.

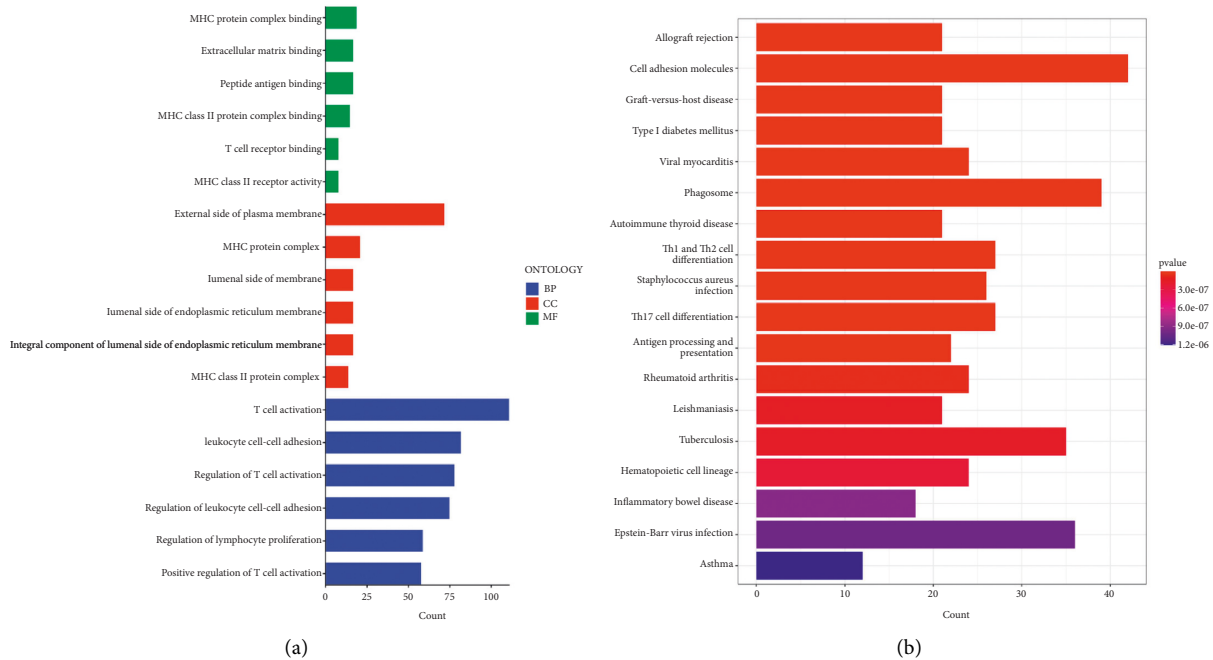


FIGURE 5: (a, b) GO and KEGG enrichment analyses ( $p < 0.05$ ).

patients in the high-risk group had a shorter survival time than patients in the low-risk group. The ROC curves demonstrated the high sensitivity and specificity of the signature for survival prediction, and the one-, three-, and five-year AUC values, respectively, were 0.974, 0.929, and 0.941 in the entire set (Figure 2(a)), 0.967, 0.886, and 0.964 in the testing set (Supplementary Figure 2(a)), and 0.974, 0.924, and 0.939 in the training set (Supplementary Figure 2(b)). And, the five-year AUC values of the model were higher than the traditional clinicopathological characteristics (Figure 2(b)).

Risk score was shown to be a significant prognostic risk factor in univariate Cox regression analysis ( $p = 0.001$ ; Figure 2(c)) and an independent prognostic risk factor in multivariate Cox regression analysis ( $p = 0.003$ ; Figure 2(d)). The risk model predicted the prognosis of UM better than other standard clinicopathological features, according to the C-index and DCA (Figures 2(e) and 2(f)). The signature and clinicopathological features nomogram was found to be trustworthy and sensitive, and it may be used to predict UM patient survival (Figure 3). The

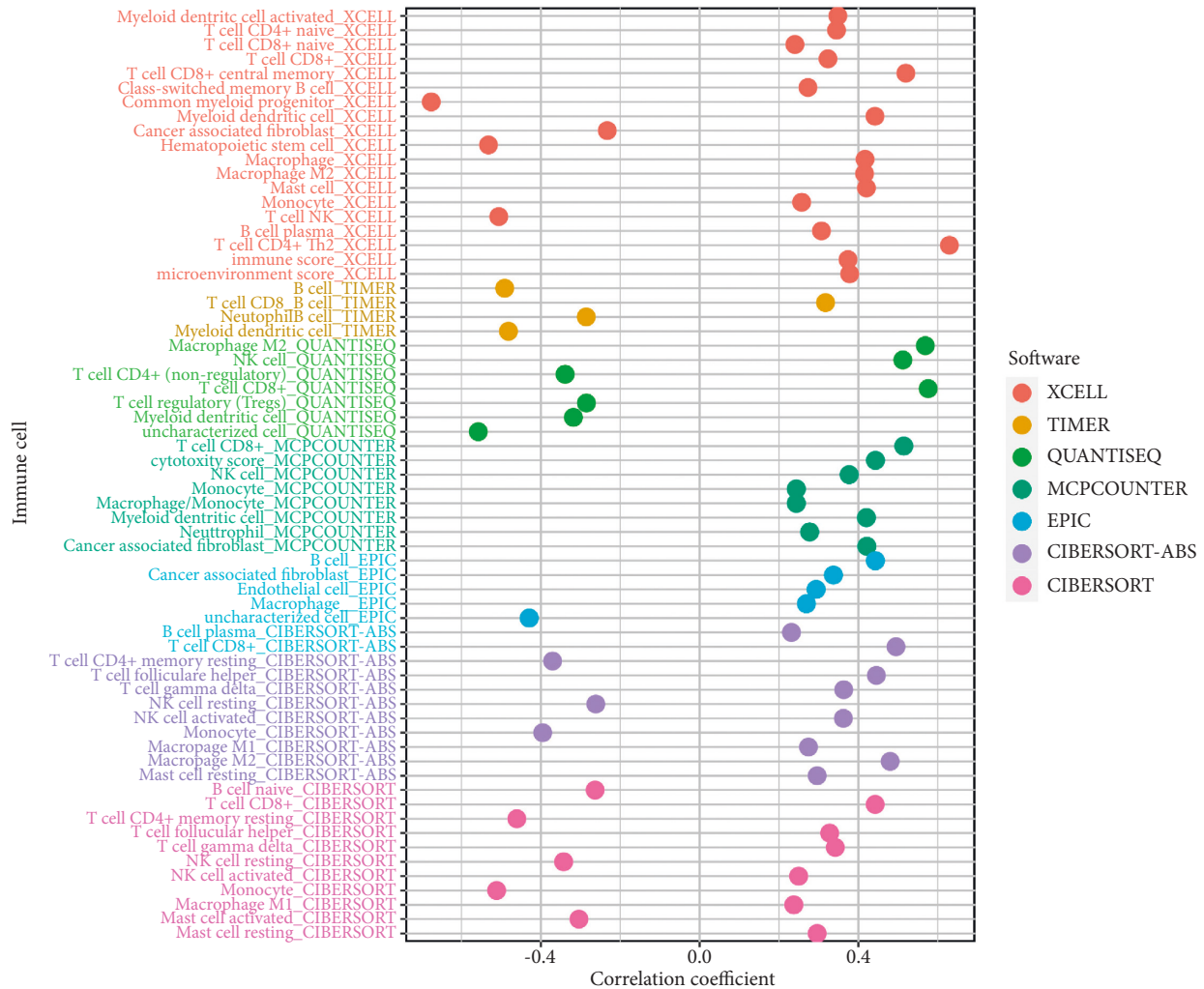


FIGURE 6: In the high-risk group, CD4+ T cells, CD8+ T cells, NK cells, M1 macrophages, M2 macrophages, myeloid dendritic cells, and fibroblasts were more abundant, whereas mast cells were more abundant in the low-risk group.

nomogram's calibration plot predicts the probability of a one-, three-, and five-year prognosis (Supplementary Figure 2(c)). PCA indicated that the distributions of entire gene expression profiles, immune-related genes, and lincRNAs between different groups were relatively scattered (Figures 4(a)–4(c)), while the distributions of 3 lincRNAs in the signature between different groups had different distributions (Figure 4(d)).

**3.4. Exploration of Functional Enrichment.** We used GO and KEGG enrichment analyses to study the underlying molecular processes of the lincRNAs model. Immune cell activation, proliferation, and adhesion, as well as MHC binding, were all shown to be involved in the GO enrichment analysis,  $p < 0.05$  (Figure 5(a) and Supplementary Table 3). Immunological system illnesses, immune responses, and immune cell differentiation were all shown to be involved in the KEGG enrichment analysis,  $p < 0.05$  (Figure 5(b) and Supplementary Table 4).

**3.5. Exploration of Immunological Atlas.** In terms of immune cell infiltration, the high-risk group had more CD4+ T cells, CD8+ T cells, NK cells, M1 macrophages, M2 macrophages, myeloid dendritic cells, and fibroblasts, whereas the low-risk group had more mast cells (Figure 6). CTLA-4 ( $p$  0.01), PDCD1 ( $p$  0.001), LAG3 ( $p$  0.001), TIGIT ( $p$  0.001), and BTLA ( $p$  0.01), among other genes, were found to be substantially different between different groups (Figure 7(a)). Apart from APC co-inhibition and type II IFN response, the bulk of immune activities were statistically distinct between different groups (Figure 7(b)). TIDE scores were higher in the high-risk group than in the low-risk group ( $p$  0.05), indicating that the high-risk group was more likely to respond to immunotherapy (Figure 7(c)).

**3.6. Recognized Potential Compounds.** Along with immunotherapy, we searched for potential compounds that target our signature for treating UM patients. Finally, we discovered that various agents (AMG.706, bicalutamide, BX.795, etc.) were identified for significant differences in the





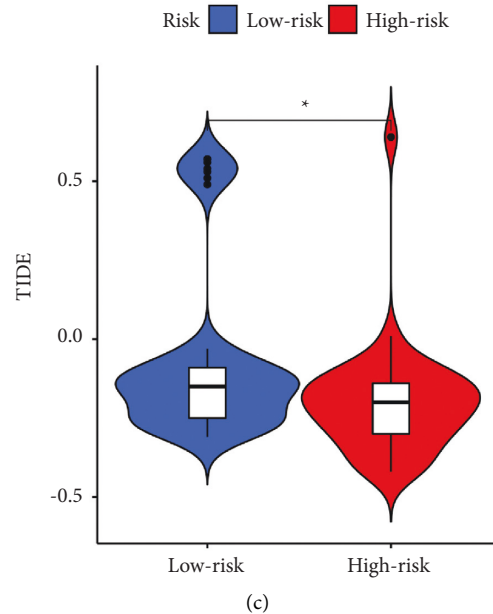


FIGURE 7: (a) Expression of the majority of ICIs-related molecules was higher in the high-risk group. (b) The majority of immune functions were statistically different between high- and low-risk groups, except for APC co-inhibition and type II IFN response. (c) TIDE scores were higher in the high-risk group.

estimated IC50 between high- and low-risk groups (Figure 8 and Supplementary Figure S3).

#### 4. Discussion

Currently, research for the UM model on the basis of lncRNAs is still scarce. Chen et al. recognized six autophagy-associated lncRNAs and constructed a signature, which can predict the prognosis of UM patients [15]. Liao et al. established an eight prognostic microenvironment-related lncRNAs signature and identified potential small molecule drugs [16]. In summary, we established for the first time a risk assessment model on the basis of irlncRNAs that can predict the prognosis and immunotherapy response in UM patients.

While immunotherapy has significantly improved the therapeutic regimens to cutaneous melanoma, its efficacy in UM has not been as dramatic. The eye is associated with many positive immunosuppressive mechanisms compared to other parts of the tissue [17–19]. Based on previous studies, lncRNAs and immune-related genes have been frequently used for model construction and subtype identification, and promising results have been observed [20–22]. We were motivated by the function of immune-related genes and lncRNAs in UM and tried to construct a prognostic risk model on the basis of irlncRNAs.

In the research, 2,216 irlncRNAs were identified to investigate the prognostic function of irlncRNAs. Then, 409 irlncRNAs were associated with prognosis, 6 candidate irlncRNAs (ELFN1-AS1, AF131216.4, AP005121.1, AC079089.1, AC104117.3, and SOX1-OT) were filtered out by LASSO, and 3 prognostic irlncRNAs were applied to construct a model. Among these 6 candidate irlncRNAs, ELFN1-AS1 was considered as an oncogene in a variety of cancers, AC079089.1,

AC104117.3, and SOX1-OT have been shown to have a function in the progression of various diseases, and other lncRNAs were first identified [23–28]. The Kaplan–Meier analysis, ROC analysis, Cox regression analysis, C-index, DCA, PCA analysis, and nomogram were applied to assess the validity and accuracy of the risk model. The results of GO and KEGG enrichment analyses indicated that the model is significantly related to immune-related pathways and molecules.

We found that CD4+ T cells, CD8+ T cells, NK cells, M1 macrophages, M2 macrophages, myeloid dendritic cells, and fibroblasts were more abundant in the high-risk group. Significantly, high lymphocytic infiltration in um is associated with poor prognosis, in agreement with our results [23–29]. We also found that the expression of most ICIs-related molecules and the scores of most immune functions were higher in the high-risk group than low-risk group. Also, TIDE scores were higher in the high-risk group than in the low-risk group. TIDE is a computational platform for immunotherapy prediction, and its predictive capabilities have been demonstrated in many cancers with great success [30–33]. These results suggest that patients in the high-risk group have a higher response rate to immunotherapy. Therefore, we believe that patients in the high-risk group might be more appropriate to receive immunotherapy. We also discovered that various drugs (AMG.706, Bicalutamide, BX.795, etc.) were identified for significant differences in the IC50 between different groups. Currently, the immune pathogenesis of UM related to immune cells, cytokines, etc., has been further understood, but they are still unclear, and no definite and effective immunotherapeutic drug has been developed so far. The immune cells and cytokines associated with UM are still unclear. Although immunotherapy with anti-CTLA4 and anti-PD-1/PD-L1 reagents has significantly

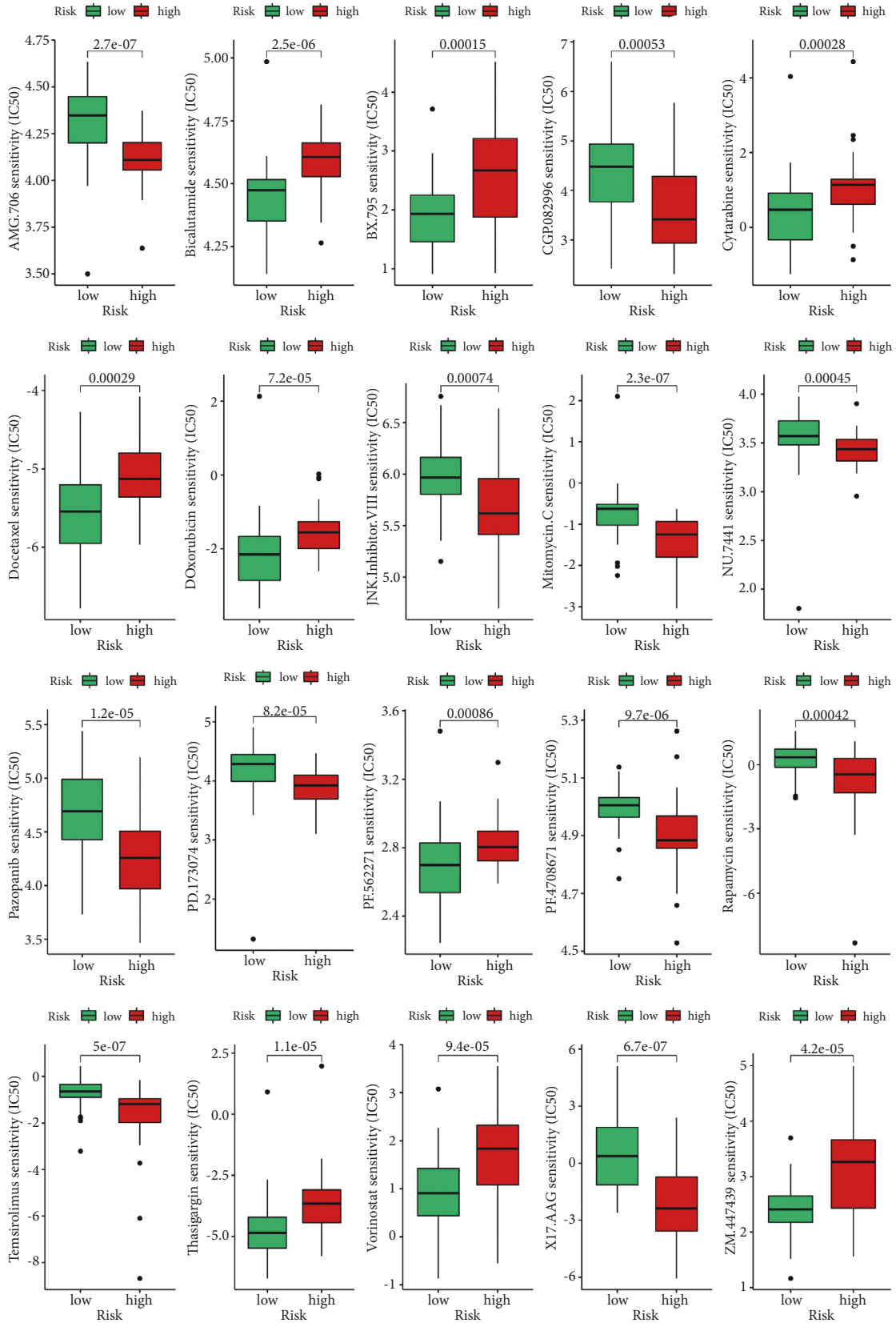


FIGURE 8: Identification of potential drugs targeting the model ( $p < 0.001$ ).

improved the treatment of metastatic cutaneous melanoma, the application in UM has not been satisfactory [34]. In addition, how to better increase M1-type TAM, promote DC maturation, and how to suppress NKT cells and activate NK cells, improve DC vaccine, etc., also need to be studied. With the increasing research in basic immunology and ophthalmology, NK cell activation, DC vaccine, and T cell relay therapy have been improved. The immunopathogenesis of UM and the related disciplines such as basic immunology and ophthalmology are developing rapidly. We believed that the research on the immunopathogenesis and immunotherapy of UM will make new breakthroughs in the future.

**4.1. Limitations.** Naturally, this study has some drawbacks and limitations. On the one hand, the UM samples extracted from the TCGA consisted of only 80 tumor samples and no normal samples, which was small and did not allow for differential expression analysis. On the other hand, the model developed in this study lacks validation by cellular experiments, animal experiments, or clinical samples. In subsequent studies, we will further expand the tumor samples, collect as many normal samples as possible, and conduct relevant experiments to follow-up our experimental findings.

## 5. Conclusions

Taken together, we constructed a new model on the basis of irlncRNAs that can precisely predict prognosis and response on immunotherapy of UM patients, which may provide worthwhile clinical applications in antitumor immunotherapy.

## Data Availability

The original contributions presented in the study are publicly available. These data can be found at <https://portal.gdc.cancer.gov> (TCGA-UM).

## Ethical Approval

All data of this study were public and required no ethical approval.

## Conflicts of Interest

The authors declare that they have no conflicts of interest.

## Authors' Contributions

Wei Chen, Liying Yan, and Bo Long wrote the manuscript, performed data extraction, and did statistical analysis. Wei Chen, Liying Yan, and Bo Long contributed equally to this work and are the co-first authors. Li Lin designed the research. All authors approved the final manuscript.

## Acknowledgments

This work was funded by the Research Project of Suining Central Hospital (grant number: 2019y41).

## Supplementary Materials

Figure S1: (a) Kaplan–Meier survival curve, the expression of the 3 prognostic irlncRNAs, patterns of survival outcome, and distribution of risk score for patients between different groups in the training set. (b) Kaplan–Meier survival curve, the expression of the 3 prognostic irlncRNAs, patterns of survival outcome, and distribution of risk score for patients between different groups in the testing set. Figure S2: (a, b): the ROC curves demonstrated the high sensitivity and specificity of the signature for survival prediction, and the one-, three-, and five-year AUC values, respectively, were 0.967, 0.886, and 0.964 in the testing set and 0.974, 0.924, and 0.939 in the training set. (c) The calibration plot of the nomogram predicting the probability of the one-, three-, and five-year prognosis. Figure S3: identification of potential drugs targeting the model ( $P < 0.05$ ). Table S1: identified 409 prognostic irlncRNAs. Table S2: the baseline features of these datasets, demonstrating no statistically significant variations in clinical features ( $p > 0.05$ ). Table S3: original data of GO. Table S4: original data of KEGG. . (*Supplementary Materials*)

## References

- [1] T. E. Schank and J. C. Hassel, "Tebentafusp for the treatment of metastatic uveal melanoma," *Future Oncology*, vol. 18, no. 11, pp. 1303–1311, 2022.
- [2] A. I. Riechardt, E. Kilic, and A. M. Jousseaume, "The genetics of uveal melanoma: overview and clinical relevance," *Klinische Monatsblätter für Augenheilkunde*, vol. 238, no. 7, pp. 773–780, 2021.
- [3] A. D. Singh, M. E. Turell, and A. K. Topham, "Uveal melanoma: trends in incidence, treatment, and survival," *Ophthalmology*, vol. 118, no. 9, pp. 1881–1885, 2011.
- [4] J. Yang, D. K. Manson, B. P. Marr, and R. D. Carvajal, "Treatment of uveal melanoma: where are we now?" *Therapeutic Advances in Medical Oncology*, vol. 10, 2018.
- [5] E. B. Souto, A. Zielinska, M. Luis et al., "Uveal melanoma: physiopathology and new in situ-specific therapies," *Cancer Chemotherapy and Pharmacology*, vol. 84, no. 1, pp. 15–32, 2019.
- [6] K. N. Smit, M. J. Jager, A. de Klein, and E. Kiliès, "Uveal melanoma: towards a molecular understanding," *Progress in Retinal and Eye Research*, vol. 75, Article ID 100800, 2020.
- [7] M. A. Ortega, O. Fraile-Martínez, N. García-Honduvilla et al., "Update on uveal melanoma: translational research from biology to clinical practice (Review)," *International Journal of Oncology*, vol. 57, no. 6, pp. 1262–1279, 2020.
- [8] R. S. Seedor, M. Orloff, and T. Sato, "Genetic landscape and emerging therapies in uveal melanoma," *Cancers*, vol. 13, no. 21, Article ID 5503, 2021.
- [9] D. B. Johnson and A. B. Daniels, "Continued poor survival in metastatic uveal melanoma: implications for molecular prognostication, surveillance imaging, adjuvant therapy, and clinical trials," *Jama Ophthalmol*, vol. 136, no. 9, pp. 986–988, 2018.
- [10] A. P. Algazi, K. K. Tsai, and A. N. Shoushtari, "Clinical outcomes in metastatic uveal melanoma treated with PD-1 and PD-L1 antibodies," *Cancer*, vol. 122, pp. 3344–3353, 2016.

- [11] T. E. Schank and J. C. Hassel, "Immunotherapies for the treatment of uveal melanoma-history and future," *Cancers*, vol. 11, no. 8, p. 1048, 2019.
- [12] K. F. Bol, E. Ellebaek, L. Hoejberg et al., "Real-world impact of immune checkpoint inhibitors in metastatic uveal melanoma," *Cancers*, vol. 11, no. 10, Article ID 1489, 2019.
- [13] P. Milán-Rois, A. Quan, F. J. Slack, and A. Somoza, "The role of lncRNAs in uveal melanoma," *Cancers*, vol. 13, no. 16, Article ID 4041, 2021.
- [14] F. J. Slack and A. M. Chinnaiyan, "The role of non-coding RNAs in oncology," *Cell*, vol. 179, no. 5, pp. 1033–1055, 2019.
- [15] Y. Chen, L. Chen, J. Wang, J. Tan, and S. Wang, "Identification of six autophagy-related-lncRNA prognostic biomarkers in uveal melanoma," *Disease Markers*, vol. 2021, pp. 1–12, 2021.
- [16] C. L. Liao, X. Y. Sun, Q. Zhou, M. Tian, Y. Cao, and H. B. Lyu, "Identification and validation of tumor microenvironment-related lncRNA prognostic signature for uveal melanoma," *International Journal of Ophthalmology*, vol. 14, no. 8, pp. 1151–1159, 2021.
- [17] J. Y. Niederkorn, "Ocular immune privilege and ocular melanoma: parallel universes or immunological plagiarism?" *Frontiers in Immunology*, vol. 3, p. 148, 2012.
- [18] R. S. Apte and J. Y. Niederkorn, "Isolation and characterization of a unique natural killer cell inhibitory factor present in the anterior chamber of the eye," *The Journal of Immunology*, vol. 156, no. 8, pp. 2667–2673, 1996.
- [19] R. S. Apte, E. Mayhew, and J. Y. Niederkorn, "Local inhibition of natural killer cell activity promotes the progressive growth of intraocular tumors," *Investigative Ophthalmology and Visual Science*, vol. 38, no. 6, pp. 1277–1282, 1997.
- [20] J. Yin, X. Li, C. Lv et al., "Immune-related lncRNA signature for predicting the immune landscape of head and neck squamous cell carcinoma," *Frontiers in Molecular Biosciences*, vol. 8, Article ID 689224, 2021.
- [21] W. F. Hong, L. Liang, Y. J. Gu et al., "Immune-related lncRNA to construct novel signature and predict the immune landscape of human hepatocellular carcinoma," *Molecular Therapy—Nucleic Acids*, vol. 22, pp. 937–947, 2020.
- [22] J. Wang, C. Shen, D. Dong, X. Zhong, Y. Wang, and X. Yang, "Identification and verification of an immune-related lncRNA signature for predicting the prognosis of patients with bladder cancer," *International Immunopharmacology*, vol. 90, Article ID 107146, 2021.
- [23] X. Jing, L. Du, S. Shi et al., "Hypoxia-induced upregulation of lncRNA ELFN1-AS1 promotes colon cancer growth and metastasis through targeting TRIM14 via sponging miR-191-5p," *Frontiers in Pharmacology*, vol. 13, Article ID 806682, 2022.
- [24] B. Yang and S. Miao, "lncRNA ELFN1-AS1 predicts poor prognosis and promotes tumor progression of non-small cell lung cancer by sponging miR-497," *Cancer Biomarkers: Section A of Disease Markers*, vol. 34, pp. 637–646, 2022.
- [25] Y. Jie, L. Ye, H. Chen et al., "ELFN1-AS1 accelerates cell proliferation, invasion and migration via regulating miR-497-3p/CLDN4 axis in ovarian cancer," *Bioengineered*, vol. 11, no. 1, pp. 872–882, 2020.
- [26] W. Feng, R. Zhu, J. Ma, and H. Song, "lncRNA ELFN1-AS1 promotes retinoblastoma growth and invasion via regulating miR-4270/SBK1 Axis," *Cancer Management and Research*, vol. 13, pp. 1067–1073, 2021.
- [27] Y. X. Chen, J. Ding, W. E. Zhou et al., "Identification and functional prediction of long non-coding RNAs in dilated cardiomyopathy by bioinformatics analysis," *Frontiers in Genetics*, vol. 12, Article ID 648111, 2021.
- [28] J. Ye, H. Li, J. Wei et al., "Risk scoring system based on lncRNA expression for predicting survival in hepatocellular carcinoma with cirrhosis," *Asian Pacific Journal of Cancer Prevention*, vol. 21, no. 6, pp. 1787–1795, 2020.
- [29] S. Feng, T. Xia, Y. Ge et al., "Computed tomography imaging-based radiogenomics analysis reveals hypoxia patterns and immunological characteristics in ovarian cancer," *Frontiers in Immunology*, vol. 13, Article ID 868067, 2022.
- [30] W. Hao, H. Zhao, Z. Li et al., "Identification of potential markers for differentiating epithelial ovarian cancer from ovarian low malignant potential tumors through integrated bioinformatics analysis," *Journal of Ovarian Research*, vol. 14, no. 1, p. 46, 2021.
- [31] Y. Zhu, S. Feng, Z. Song, Z. Wang, and G. Chen, "Identification of immunological characteristics and immune subtypes based on single-sample gene set enrichment analysis algorithm in lower-grade glioma," *Frontiers in Genetics*, vol. 13, Article ID 894865, 2022.
- [32] S. L. Topalian, J. M. Taube, R. A. Anders, and D. M. Pardoll, "Mechanism-driven biomarkers to guide immune checkpoint blockade in cancer therapy," *Nature Reviews Cancer*, vol. 16, no. 5, pp. 275–287, 2016.
- [33] F. Xu, X. Huang, Y. Li, Y. Chen, and L. Lin, "m6A-related lncRNAs are potential biomarkers for predicting prognoses and immune responses in patients with LUAD," *Molecular Therapy—Nucleic Acids*, vol. 24, pp. 780–791, 2021.
- [34] I. Pires da Silva, T. Ahmed, I. L. M. Reijers et al., "Ipilimumab alone or ipilimumab plus anti-PD-1 therapy in patients with metastatic melanoma resistant to anti-PD-(L)1 monotherapy: a multicentre, retrospective, cohort study," *The Lancet Oncology*, vol. 22, no. 6, pp. 836–847, 2021.